Molecular Dynamics Simulations of HMX Crystal Polymorphs Using A Flexible Molecule Force Field

Dmitry Bedrov,* Chakravarthy Ayyagari, and Grant D. Smith

Department of Materials Science and Engineering and
Department of Chemical & Fuels Engineering
122 S. Central Campus Drive, Room 304
University of Utah
Salt Lake City, UT 84112

Thomas D. Sewell and Ralph Menikoff

Theoretical Division
Los Alamos National Laboratory
Los Alamos, NM 87545

Joseph M. Zaug

Lawrence Livermore National Laboratory
7000 E. Ave., L-282
Livermore, CA 94551

LAUR-00-2377

Abstract

Molecular dynamics simulations using a recently developed quantum chemistry-based atomistic force field [*J. Phys. Chem. B*, **1999**, *103*, 3570] were performed in order to obtain unit cell parameters, coefficients of thermal expansion, and heats of sublimation for the three pure crystal polymorphs of octahydro-1,3,5,7-tetranitro-1,3,5,7-tetrazocine (HMX). The predictions for β-, α-, and δ-HMX showed good agreement with the available experimental data. For the case of β-HMX, anisotropic sound speeds were calculated from the molecular dynamics

simulation-predicted elastic coefficients and compared with recent Impulsive Stimulated Light Scattering (ISLS) sound speed measurements. The level of agreement is encouraging.

Introduction

Plastic-bonded explosives (PBXs) are composites comprised of high-explosive crystallites held together by a polymeric binder. Mesomechanical simulation methods, in which the individual explosive grains are resolved within a continuum hydrodynamic framework, are being used to understand ignition and assess the sensitivity of PBXs to various stimuli.[1] Though there are data on bulk properties, simulations on the grain scale require thermophysical and mechanical properties of a single crystal of explosive. Many of these properties are difficult to measure due to the extremely rapid decomposition that occurs for the pressure and temperature regions of interest. Fortunately, judicious application of molecular simulation tools provides a viable path to determine many of the grain-scale properties needed for mesomechanical models.

Octahydro-1,3,5,7-tetranitro-1,3,5,7-tetrazocine (HMX) is the energetic component in several important high-performance PBXs, e.g., PBX-9501.[2] We have previously reported values for temperature-dependent density and equilibrium transport coefficients of liquid HMX at atmospheric pressure in the domain 550 K ≤ T ≤ 800 K.[3,4] The predictions were obtained from multi-nanosecond molecular dynamics (MD) simulations using a recently published, fully flexible, quantum chemistry-based atomistic force field for HMX. [5] Our initial focus on liquid transport coefficients was motivated by the needs of mesomechanics modelers since there were no direct determinations, either experimental or theoretical, for those parameters. In this paper we present results of MD simulations using the same force field for the three pure crystal polymorphs of HMX. The β-, α-, and δ- phases of HMX are monoclinic[6] ($P_{21/n}$ spacegroup, Z=2

molecules per unit cell, symmetry axis = *b*), orthorhombic[7] (F*dd*2, Z=8), and hexagonal[8] ($P6_1$, Z = 6, symmetry axis = *c*), respectively. The primary purpose of this work is to validate the force field against the available experimental data for HMX.

Force Field and Simulation Protocol

The force field has been described previously[5] and was used without modification in the present study with the exception that partial atomic charges were increased by 25% in order to take into account the polarization effects in the condensed phases; these scaled charges were also used in Refs. 3 and 4. In our previous simulations of dimethylnitramine[9] we found that the increase of partial atomic charges by 25% yielded density and cohesive energy in good agreement with experiment. As in our previous studies,[3,4] the covalent bonds were held fixed to constant values determined from quantum chemistry calculations. Since the bond lengths in the force field are constrained, the small differences in lengths observed for chemically similar bonds in the various polymorphs - as well as within a single molecule in a given polymorph - will not be reproduced in our calculations. However, the effects of this on our results are expected to be minor. Moreover, the measured unit cell volumes are predicted quite accurately by the present force field, as shown below. Isothermal-isobaric (*NpT*) molecular dynamics simulations[10] were performed at atmospheric pressure for each phase using the Rahman-Parrinello approach,[11] with primary simulation cells corresponding to 24 (4 x 2 x 3), 8 (2 x 1 x 4), and 16 (4 x 4 x 1) unit cells for β-, α- and δ-HMX, respectively. A systematic investigation of the influence of frequencies for the barostat (w_b) and thermostat (w_t) on the volume and enthalpy fluctuations was performed to determine a range of these frequencies for which the fluctuations are independent of the values chosen; values of w_b=8.0x10^{-4} fs^{-1} for barostat and w_t=1.0x10^{-2} fs^{-1} for thermostat were used for all simulations reported here. Experimental crystal structures[6,7,8]

were used to define initial configurations for the simulations. For each system, an equilibration run of 0.5 ns duration was performed, followed by a 1.0 ns production run; the integration step size and sampling interval were 1 fs and 10 fs, respectively. In order to provide sufficient sampling of strain-strain fluctuations, a 5.0 ns production run was generated for the β-HMX system at 295 K. Nonbonded interactions were truncated at 10.0 Å; the standard Ewald summation[12] was used to handle long-range electrostatics. Intramolecular bond lengths were constrained using the SHAKE algorithm.[13]

Results and Discussion

Cell parameters. In Table 1 we report atmospheric pressure lattice parameters and unit cell volumes for β–, α–, and δ-HMX as obtained from MD simulations at 295 K. Also shown for comparison are the experimental data obtained at 295 K. It can be seen that the simulation results are in good agreement with experiment. The largest percent error in unit cell volume, 1.4%, occurs for α-HMX. The lattice angles are essentially exact with the exception of β-HMX, for which the angle β is 3.6% too small. This error is compensated by errors of –4.7% and 3.7% in lattice lengths *b* and *c*, respectively, to yield nearly perfect agreement with experiment for the unit cell volume. **(**The errors in those two lattice parameters are the largest obtained in the present work.) Overall, the current predictions are more accurate than those based on the force field of Dzyabchenko *et al*.[14] and comparable to those reported by Sorescu *et al.* [15] More detailed comparisons among the force fields are somewhat problematic, however, since in the former case molecular packing was used while in the latter case the temperatures at which the isothermal-isobaric calculations were performed for α- and δ-HMX did not correspond to those for which experimental structural determinations have been reported (295 K).

Coefficients of Thermal Expansion. In order to determine the coefficients of thermal expansion (CTEs), simulations for each polymorph were performed at several temperatures in the associated stability domains,[16] as well as at 295 K; we used 250 < *T* < 350 K (250, 280, 295, 320, and 350 K) for β-HMX, 295 < *T* < 450 K (295, 350, 380, 400, 420, and 450 K) for α-HMX and 295<*T*<520 K (295, 480, 500, and 520 K) for δ-HMX. The resulting temperature dependencies of the lattice parameters were adequately described by straight lines; thus, the CTE χ_X for a given lattice parameter at 295 K was determined from $\chi_{X,295K}=1/X_{295K}(\partial X/\partial T)$ where X=*a*, *b*, *c*, and *V*. The CTEs thus obtained are reported in Table 1 and are in generally good agreement with the experimental data at 295 K,[17,18] which are included for comparison. The largest deviation of the predicted χ_V from experimental data is observed for β-HMX and is 11.4%. The CTEs of the individual cell parameters are in best agreement with experiment for α- and δ-HMX, and somewhat less so for β-HMX.[19] In Figure 1 we compare CTEs predicted in this work with experimental data[17,18] and from previous simulations with a rigid molecule force field.[15] The current CTEs are of comparable or even better accuracy than the values obtained from the rigid-molecule force field.

Enthalpy of Sublimation. The accuracy with which a force field predicts enthalpies of sublimation is another crucial test of its overall validity. The sublimation enthalpy can be determined as:

$$\Delta H_s = H_{gas} - H_{solid} = RT + \Delta E_{inter} + \Delta E_{intra} \qquad (1)$$

where ΔE_{inter} and ΔE_{intra} are the differences in intermolecular and intramolecular potential energies of HMX molecules in the ideal gas and relevant crystal phases, respectively. We note that for HMX ΔE_{intra} is not negligible: quantum chemistry calculations[5] at the B3LYP/6-311G** level indicate that the energy difference between the lowest energy gas-phase geometry and that

of an optimized gas-phase molecule in the nominal α-HMX conformation is 3.5 kcal/mol. Also, in the crystal phase, bends and torsions of a particular conformer can be distorted from the optimal values of the corresponding gas-phase conformer due to condensed-phase effects. While the difference in intramolecular energies of gas- and solid-phase molecules can make a significant contribution to ΔH_s, this effect has been ignored in the assessment of other force fields.[14,15] In order to obtain the intramolecular energy difference in the present work, simulations of an HMX ideal gas were performed at 295 K using a stochastic dynamics algorithm described elsewhere.[20] The calculated sublimation energies for each polymorph are provided in Table 1, where they are compared (for β- and δ-HMX) to values derived by Lyman *et al.*[21] based on a combined analysis of experimental data due to others.[22,23] Good agreement between experimental and MD predicted enthalpies is obtained. The predicted ΔH_s for α-HMX lies in between the values of β- and δ-HMX, which is consistent with the polymorph stability ranking[16] ($\beta > \alpha > \delta$) at room temperature. The ΔE_{inter} and ΔE_{intra} contributions to ΔH_s obtained from MD simulations are also reported in Table 1. ΔE_{intra} makes an important contribution to the ΔH_s of α- and δ-HMX (7.0 and 10.0 kcal/mol, respectively) and is only about 0.8 kcal/mol for β-HMX. It is worth noting that the polymorph dependence of the intermolecular energy contribution to ΔH_s is opposite to that of ΔH_s itself, *i.e.*, the intermolecular interactions for δ- and α-HMX are more favorable than for β-HMX. However, this relative "stabilization" of δ- and α-HMX due to intermolecular interactions is compensated by the unfavorable intramolecular energy of HMX molecules in these phases, resulting in smaller enthalpies of sublimation relative to β-HMX.

Sound Speeds. An elastic material has three acoustic sound speeds, corresponding to one quasi-longitudinal and two quasi-transverse waves. The speeds depend on the direction of propagation. For a given direction $\hat{\mathbf{n}}$ the speeds are determined by the equation[24]

$$\det\left(n_i C_{ijkl} n_l - \rho c^2 \delta_{jk}\right) = 0, \tag{2}$$

where ρ is the density, C_{ijkl} is the fourth-rank elastic tensor, c are the sound speeds, and δ_{jk} is the Kronecker delta symbol. We have calculated the elastic coefficients for β-, α-, and δ-HMX at 295 K from our MD simulations[25] by application of the strain-strain fluctuation formula due to Rahman and Parrinello[26]:

$$C_{ijkl} = \frac{\kappa T}{\langle V \rangle} \left\langle \varepsilon_{ij} \varepsilon_{kl} \right\rangle^{-1}, \tag{3}$$

where $\langle \varepsilon_{ij} \varepsilon_{kl} \rangle$ is the fluctuation of the second-rank elastic strain tensor, and $\langle V \rangle$ is the average volume of the simulation cell. The strain fluctuation is readily constructed from a suitably large set of observations of the crystal lattice parameters sampled over the course of a *NpT* molecular dynamics trajectory. Details of these procedures can be found elsewhere.[27,28] The elastic coefficients determined from our simulations were used to predict the quasi-longitudinal and quasi-transverse sound speed curves. In Figure 2 the sound speeds for β-HMX, obtained (1) from direct Impulsive Stimulated Light Scattering (ISLS) measurements[29] and (2) using the elastic coefficients determined from our MD simulations, are compared for propagation in the plane normal to the crystal symmetry axis. We point out that the MD simulations determine isothermal sound speeds while the measurements correspond to isentropic conditions. However, the difference between the two is expected to be small.[25] Good agreement (to within ~10%) is obtained for the quasi-longitudinal component, although there is a small shift in the locations of

the extrema along the abscissa. There are only a few data points for the quasi-transverse sound speeds and their polarization was not determined in the experiments. Regardless, the level of agreement for this case appears to be less satisfactory than for the quasi-longitudinal component. More experimental data would be required to fully assess the accuracy of our predictions for the quasi-transverse sound speeds.

Conclusions

We have used a quantum chemistry-based intra- and intermolecular force field to predict the crystal structures, coefficients of thermal expansion, and heats of sublimation of the three pure polymorphs of HMX; and the sound speeds of β-HMX at 295 K; all at atmospheric pressure. The results for the lattice parameters and their temperature dependencies are in good agreement with experiment. The predicted enthalpies of sublimation are consistent with experimental measurements. Direct comparison between measured and predicted anisotropic sound speeds for β-HMX reveals good agreement for the quasi-longitudinal component. Overall, the simulations using the quantum chemistry-based force field predict properties of HMX crystal polymorphs that are in good agreement with the available experimental data. This validates the force field and provides increased confidence for its use in simulations of HMX at thermodynamic states for which experimental data are difficult, if not impossible, to obtain. These simulations are currently underway.

Acknowledgments

CA, DB and GDS are funded by the University of Utah Center for the Simulation of Accidental Fires and Explosions (C-SAFE), funded by the Department of Energy, Lawrence Livermore National Laboratory, under subcontract B341493. TDS and RM are supported by the Los

Alamos ASCI High Explosives Effort. JMZ wishes to thank Philip M. Howe (Los Alamos) for support during the time the experiments were carried out, and the University of Washington (Profs. L.J. Slutsky and J.M. Brown) for the use of laboratory facilities.

References

(1) For example, Menikoff, R. *Granular Explosives and Initiation Sensitivity*, LA-UR-996023. http://t14web.lanl.gov/Staff/rsm/preprints.html#Initiation.

(2) *LASL Explosive Property Data*, Eds. Gibbs, T.R.; Popolato, A. (University of California, Berkely, 1980).

(3) Bedrov, D.; Smith, G.D.; Sewell, T.D. *J. Chem. Phys.* **2000**, *112*, 7203.

(4) Bedrov, D.; Smith, G.D.; Sewell, T.D. *Chem. Phys. Lett.* **2000**, *324*, 64.

(5) Smith, G.D.; Bharadwaj, R.K. *J. Phys. Chem. B* **1999**, *103*, 3570.

(6) Kohno, Y.; Maekawa, K.; Azuma, N.; Tsuchioka, T.; Hashizume, T.; Imamura, A. *Kogyo Kayako* **1992**, *53*, 227.

(7) Cady, H.H.; Larson, A.C.; Cromer, D.T. *Acta Cryst.* **1963**, *16*, 617.

(8) Cobbledick, R.E.; Small, R.W.H. *Acta Cryst. B* **1974**, *30*, 1918.

(9) Smith, G.D.; Bharadwaj, R.K.; Bedrov, D.; Ayyagari, C. *J. Phys. Chem. B* **1999**, *103*, 705.

(10) Martyna, G.J.; Tuckerman, M.E.; Tobias, D.J.; Klein, M.L. *Mol. Phys*. **1996**, *87*, 1117.

(11) Parrinello, M.; Rahman, A. *J. Appl. Phys*. **1981**, *52*, 7182.

(12) Allen, M.P.; Tildesley, D.T. *Computer Simulation of Liquids* (Oxford, NY, 1987).

(13) Ryckaert, J.; Ciccotti, G.; Berendsen, H.G.C. *J. Comp. Phys*. **1977**, *23*, 327.

(14) Dzyabchenko, A.V.; Pivina, T.S.; Arnautova, E.A. *J. Mol. Structure* **1996**, *378*, 67.

(15) Sorescu, D.C.; Rice, B.M.; Thompson, D.L. *J. Phys. Chem. B* **1998,** *102***,** 6692.

(16) McCrone, W.C. In *Physics and Chemistry of the Organic Solid State*; Fox, D.; Labes, M.M.; Weissberger, A.; Eds.; (Wiley, NY, 1965; Vol. II.)

(17) Herrmann, M.; Engel, W.; Eisenreich, N. *Propellants Explosives Polytechnics* **1992**, *17*, 190.

(18) Herrmann, M.; Engel, W.; Eisenreich, N. *Z. Kristall*. **1993**, *204*, 121.

(19) We note that the linear and volumetric CTEs in Refs. 17 and 18 are not self-consistent in that the latter do not follow from the former according to the formal expression (for a monoclinic

cell) $\chi_V=\chi_a+\chi_b+\chi_c+(\cos\beta/\sin\beta)\beta\chi_\beta$. . The reason for this is that χ_V was determined from a direct fit to the temperature dependent unit cell volume rather than from the linear CTEs (M. Herrmann, private communication). Although the same approach was used here, we obtained self-consistency to the percent level.

(20) Smith, G.D.; Yoon, D.Y.; Jaffe, R.L. *Macromolecules* **1993**, *26*, 298.

(21) Lyman, J.L.; Liau, Y-C.; Brand, H.V. *Combustion and Flame* submitted.

(22) Rosen, J.M.; Dickinson, C. *J. Chem. & Eng. Data* **1969**, *14*, 120.

(23) Taylor, J.W.; Crookes, R.J. *J. Chem. Soc., Faraday Trans.* **1976**, *72*, 723.

(24) Landau, L.D.; Lifschitz, E.M. *Theory of Elasticity* (Pergammon Press, Oxford, 1970), subsection 23.

(25) Sewell, T.D.; Menikoff, R.; Bedrov, D.; Smith, G.D. *J. Appl. Phys*. submitted.

(26) Parrinello, M.; Rahman, A. *J. Chem. Phys*. **1982**, *76*, 2662.

(27) Bennett, C.M.; Sewell, T.D. *J. Appl. Phys.* **2000**, 88, 88.

(28) Tsai, S.W. *Mechanics of Composite Materials*, Part II, Theoretical Aspects, AFML Tech. Rept. AFML-TR-66-149, November 1966.

(29) Zaug, J.M. "Elastic Constants of β-HMX and Tantalum, Equations of State of Supercritical Fluids and Fluid Mixtures and Thermal Transport Determinations" to appear in *Proceedings of the Eleventh Symposium (International) on Detonation*, Snowmass, Colorado, U.S.A., **1998**.

Table 1. Properties of HMX polymorphs from MD simulations[a] and experiments at 295 K.

Property	β-HMX		α-HMX		δ-HMX	
	MD	expt	MD	expt	MD	expt
a [Å]	6.5306	6.5347[b]	14.9912	15.14[e]	7.6200	7.711[f]
b [Å]	10.5086	11.0296[b]	23.9080	23.89[e]	7.6100	7.711[f]
c [Å]	7.6246	7.3549[b]	6.0531	5.913[e]	33.5340	32.553[f]
α	89.999	90.0[b]	89.990	90.0[e]	89.999	90.0[f]
β	98.946	102.69[b]	90.000	90.0[e]	89.994	90.0[f]
γ	90.000	90.0[b]	89.999	90.0[e]	120.170	120.0[f]
volume [Å^3]	516.86	517.16[b]	2168.86	2138.7[e]	1681.85	1676.3[f]
χ_a x10^5 [K^{-1}]	2.07	-0.29[c]	3.65	3.65[c]	4.02	4.1[c]
χ_b x10^5 [K^{-1}]	7.2	11.6[c]	4.26	4.86[c]	4.19	4.1[c]
χ_c x10^5 [K^{-1}]	2.56	2.30[c]	1.44	1.21[c]	3.94	2.6[c]
χ_V x10^5 [K^{-1}]	11.60	13.1[c]	9.34	9.6[c]	12.76	13.5[c]
ΔH_s [kcal/mol]	45.5	44.16[d]	44.2	---	41.0	42.04[d]
ΔE_{inter} [kcal/mol]	48.0		53.0		53.0	
ΔE_{intra} [kcal/mol]	-0.8		-7.0		-10.0	

[a] The first uncertain digit is the last one shown, corresponding to the standard deviations of the mean among contiguous 100 ps subaverages along the overall trajectory.
[b] Ref.[6]; [c] Refs.[17,18]; [d] Ref.[21]; [e] Ref.[7]; [f] Ref. [8].

Figure Caption

Fig. 1 Linear and volumetric coefficients of thermal expansion $\chi_{x,295K}$ for β-, α-, and δ-HMX are compared to experimental results (Refs. 17 and 18) and predictions of a rigid molecule force field (Ref. 15).

Fig. 2 Sound speeds for β-HMX in the plane normal to the symmetry axis are shown. Symbols: measured components; lines: MD predictions. Error bars on the MD predictions represent one standard deviation of the mean, and were determined on the basis of sound speeds obtained from ten independent sets of C_{ij} from contiguous 0.5 ns trajectory segments.

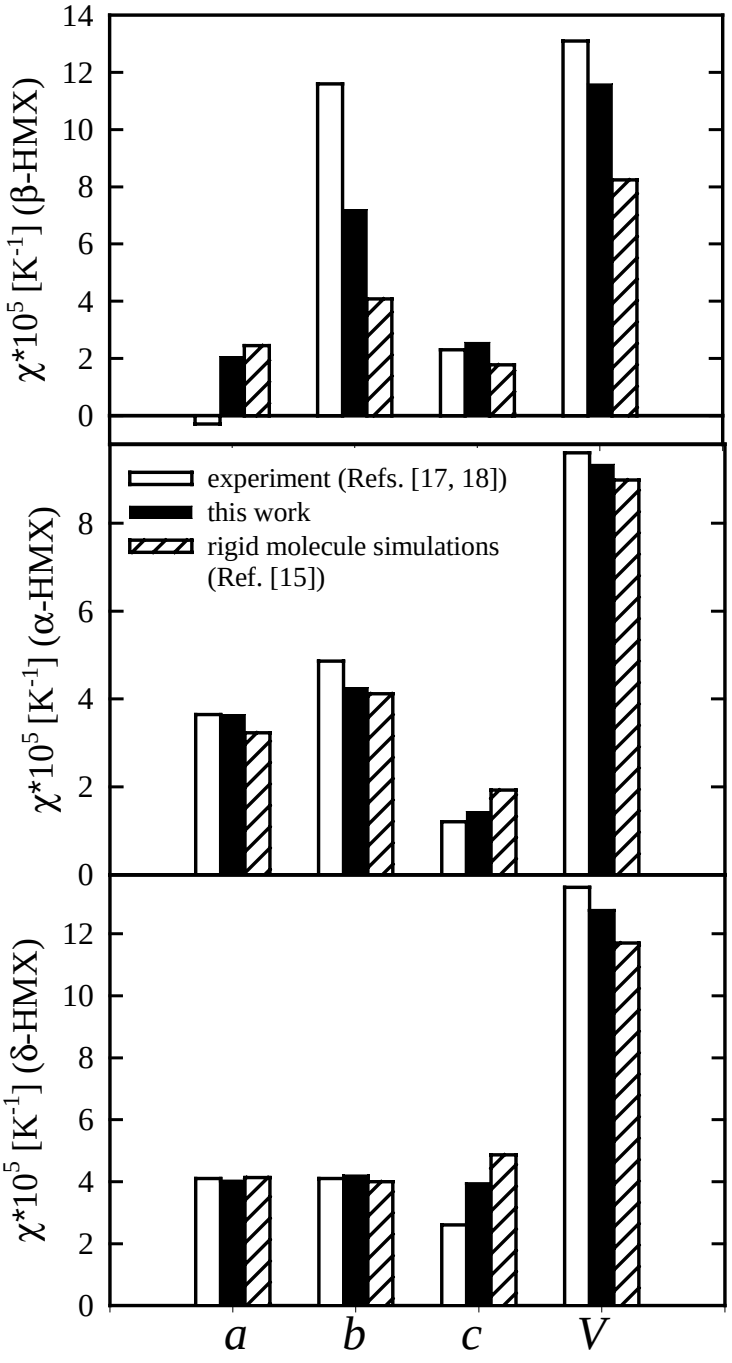
14
12
10
8
6
4
2
0
χ*10^5 [K^-1] (β-HMX)
experiment (Refs. [17, 18])
this work
rigid molecule simulations
(Ref. [15])
8
6
4
2
0
χ*10^5 [K^-1] (α-HMX)
12
10
8
6
4
2
0
χ*10^5 [K^-1] (δ-HMX)
a
b
c
V

Figure 1.

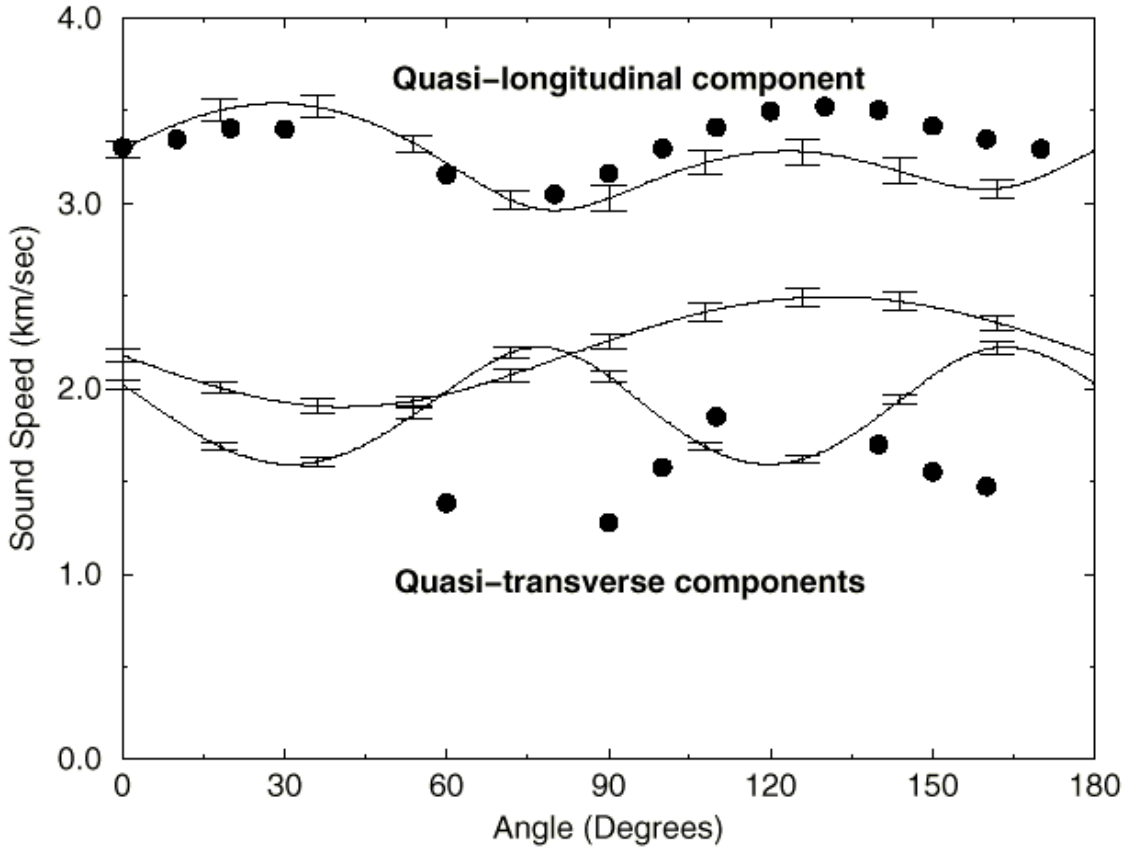
Quasi−longitudinal component
Quasi−transverse components
Sound Speed (km/sec)
Angle (Degrees)
4.0
3.0
2.0
1.0
0.0
0
30
60
90
120
150
180

Figure 2